International Journal of Engineering & Technology, 7 (4.42) (2018) 168-171

International Journal of Engineering & Technology

Website: www.sciencepubco.com/index.php/IJET

Research paper



Biomechanical Analysis of Stem Malalignment in Resurfacing Hip Arthroplasty

Shahrul Hisyam Marwan[1*], Nor Aiman Nor Izmin[2], Muhaimin Berhan[2], Abdul Halim Abdullah[2]

[1]*Faculty of Mechanical Engineering Universiti Teknologi MARA, Bukit Besi, Terengganu, Malaysia*
[2]*Faculty of Mechanical Engineering Universiti Teknologi MARA, 40450 Shah Alam, Malaysia*
**Corresponding author E-mail: shahrulhisyam@tganu.uitm.edu.my*

Abstract

Hip resurfacing arthroplasty was developed as an alternative surgical procedure to total hip arthroplasty. In this procedure, the femoral head is not removed; instead it is cut or trimmed and then capped with a metal cap. This procedure is not new news in surgery; it has been performed since the early 1970's. Basically, there are common complications between these two procedures which are fracture, malalignment of implant, bleeding and dislocation. Thus, in this study, the malalignment of implant was found to often occur in different conditions such as varus, valgus, anterversion and retroversion conditions. The objective of this study was to develop the finite element models of Hip Resurfacing Arthroplasty, to investigate the biomechanical behavior of hip arthroplasty and to examine the effects of implant malalignment as to predict the stability of the femoral component. The analyses were done under the loading conditions during normal walking for five cases of implant malalignment which were varus, valgus, sagittal extended and sagittal flexed. Both the femur and implant were developed and analyzed using computational software, namely ABAQUS 6.13. This study demonstrates that resurfacing arthroplasty will have harmful biomechanical effects when the implants are misaligned during the procedure.

Keywords: *Hip; Resurfacing; Finite Element; Femoral Head; Implant Malalignment*

1. Introduction

Hip resurfacing arthroplasty (HRA) and total hip arthroplasty (THA) are mutual procedures for patients with progressive hip osteoarthritis [1]. THA is one of the most generally performed in orthopedic procedures [2]. HRA or also known as femoral head resurfacing is like the normal proximal femoral anatomy. It has considerable advantages compared to THA which includes minimal bone loss, manageable revision and maintenance of physiological stress within the femur [3]. Prior hip resurfacing implants are endured from poor manufacturing quality, which resulted to osteolysis and aseptic loosening [4]. Nonetheless, modern advancement of this procedure which is metal-on-metal hip resurfacing arthroplasty looks as if it has solved the problems of poor materials and manufacture, producing analytical results compared to conventional total hip arthroplasty [5,6]. Hip resurfacing arthroplasty also has few complications, which are commonly stem malalignment, cup malalignment, metal sensitivity, femoral component loosening and neck fracture of the femoral component. These complications went on to be commonly reported and the main reasons for modifications. However, implant alignment has been implied as a risk factor for femoral neck fracture. Thus, the main objective of this study is to analyze and compare the results from finite element models of HRA-implanted femur, and to study the effect of different implant alignments.

2. Material and method

2.1. Material Properties

This study involved two different materials in the presentation for the malalignment of HRA effect. Hence, the femoral component used Cobalt chromium alloy (CoCr) while the femur component used cortical bone as the material. These materials are considered to be used because they have excellent biocompatibility properties. Other than that, Cobalt-chrome is also considered to have a hard-smooth durable surface. Besides, due to its relatively high hardness, high stiffness and excellent damage resistance properties, Cobalt Chromium alloy usage has widespread in the modern-day orthopaedics as a bearing surface especially in joint arthroplasty. Thus, due to its material properties, Cobalt Chromium can be used to produce very thin metallic devices without the risk of fracture. This makes it attractive for the use in hip arthroplasty procedure for active patients to conserve bone implants while maximizing the size of bearing diameter to reduce the risk of dislocation. Table 1 lists the different material properties.

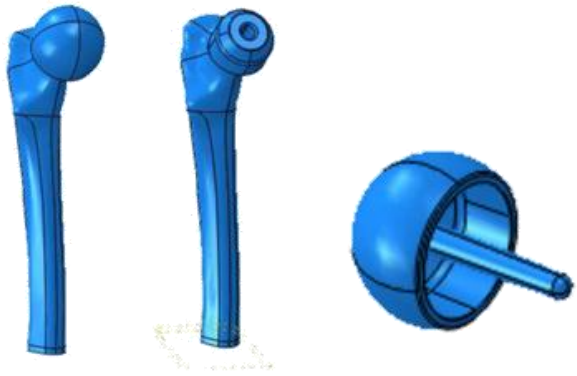
Table 1: Material Properties used for the Analysis in ABAQUS 6.13 Software. [11]

Material	Elastic Modulus (GPa)	Poisson's Ratio	Yield Strength (MPa)
Cobalt chromium (CoCr)	230	0.3	455
Cortical Bone	17	0.33	115

Copyright © 2018 Authors. This is an open access article distributed under the Creative Commons Attribution License, which permits unrestricted use, distribution, and reproduction in any medium, provided the original work is properly cited.

2.2. Femoral Component and Femur Design Model

In this project, the half femur was decided to be used because it was more convenient to complete the analysis compared to the full femur and all of the designs and analysis steps were carried out in ABAQUS 6.13 software. Previous researchers have proved this as they have completed their analysis by using the half femur as the femur component. The design of the femur actually follows the true human femur because to generate this design, it needs to approximately 3D-scan the size, shape and body structure of the actual human femur. Meanwhile, the constructed femur component has followed the standard design and size of the implant specification which was then created in CATIA software and imported to ABAQUS 6.13 software. The specification of the femoral component is listed as below in Figure 2. The length of the bridging cup is 68mm and the diameter of the femoral head is 50mm where these two component's dimensions followed the range and guideline of Birmingham resurfacing implant [5]. Fig. 1 shows the 3D model of the implant component, half femur and femoral component of hip arthroplasty.



(a) (b) (c)

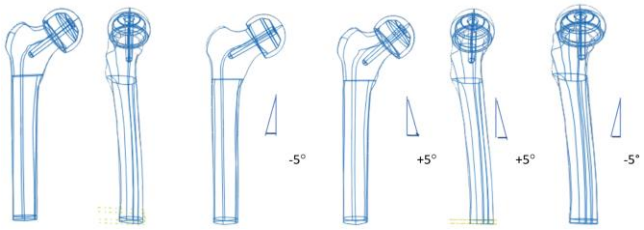
Fig. 1: 3D model of (a) half femur, (b) femur component, (c) femoral component

2.3. Different type of malalignment conditions

Finite element models of the femur and implant were generated from computed tomography CT scans of a normal hip; hence lofted to form a 3-dimensional solid model of the femur using Mechanical Finder 2.0 [7] and designed the implant using CATIA software respectively. Material parameters for the bone and implant were assigned in ABAQUS software. Five different implanted models were developed to simulate a neutrally aligned implant (125° neck-shaft angle), in 120° and 130° varus, sagittal flexed +5° and sagittal extended -3°. Meshes of each five types of RHA models were also generated and simulated in ABAQUS software to study the effect of malalignment for normal walking conditions for finite element analysis. Principal stress or von misses stress and total deformation in the half femur and implant were compared among all models to determine failure risk. These HRA models were meshed with the size of 2mm and tetrahedral elements for all models.

Table 2: The number of mesh elements in HRA models

Malalignment cases	Straight 125°	Varus -5°	Varus +5°	Sagittal flexed +5°	Sagittal extended -5°	Half femur
Femoral bone	287,664	291,552	283,574	292,346	230,226	259,877
Prosthesis stem implant	39,907	39,907	39,907	39,907	39,907	-



(a) (b) (c) (d) (e)

Fig. 2: Different type of malalignment, (a) neutrally aligned 125°, (b) varus -5°, (c) varus +5°, (d) sagittal flexed +5°, and (e) sagittal extended -5°.

2.4. Loading and boundary conditions

In this research, the 3D dimension of the femur component was generated from computed tomography CT scans of a normal hip; hence lofted to form a 3-dimensional solid model of the femur using Mechanical Finder 2.0. Meanwhile, the model for femoral component was developed in CATIA V5 software. Both components were then imported to ABAQUS 6.13 software to generate the assembly of the model, meshing and thus running the finite element analysis of the hip joint. The artificial hip joint model is shown in Fig. 3. After generating the assembly, the material properties were assigned to the respected component which was cortical bone for the femur component and cobalt-chromium for the implant component of this study. The loading analysis was conducted referring to the loading conditions of normal walking [8]. The nominal load was directed at the centre of the shell of the femoral component. The load was broken into three axes (x, y and z-axes) as the model of the HRA was developed in three dimensional. The respective loads are shown in the table below. According to HIP'98 software by Bergmann, the body weight needs to be taken into consideration to perform the finite element analysis. Thus, the considered body weight for this analysis was 836N.

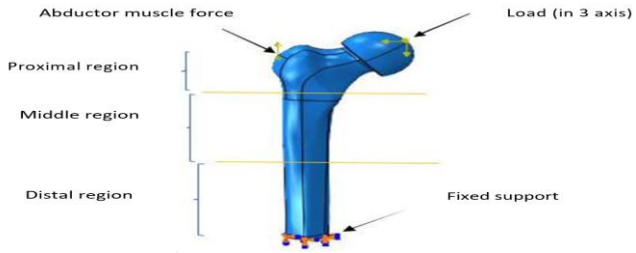


Fig. 3: An illustration of the loading conditions of the HRA model for normal walking.

Table 3: The maximum loading and abductor muscle force acted during walking

Direction	F_X	F_Y	F_Z	Resultant F
Maximum Load (N)	707.27	236.33	2085.57	2214.88
Abductor muscle(N)	475.68	19.23	726.48	868.57

3. Result and discussion

3.1. Effect of stem malalignment on Von misses stress during loading transfer of HRA

3.1.1. Hip Resurfacing Arthroplasty

This study focused on finite element analysis. Based on past research, the femoral head was assumed to be perfectly bonded to the uncemented HRA models, and the stem was also assumed to be perfectly bonded [9]. The von misses stress in all five models was compared to the natural or unimplanted hip model. Thus, the joint load for normal walking was directed to the centre of the

outer region of the acetabular cup while the end of the femur at the distal region was fixed. The body weight of the patient used to run the analysis was 836N which was referred to in HIP '98 software. The body weight is very crucial to the analysis because it affects the hip load and abductor muscle forces. From the result obtained, the varus -5° model has the highest von misses stress which is 18.83 MPa with respect to normal walking activity. The grey-coloured contour in the stress distribution indicates the maximum value of the von misses stress. It can also be seen that the sagittal flexed +5° model shows the least stress value compared to other HRA models. Hence, it can be said that it has better stability and the lowest risk of fracture.

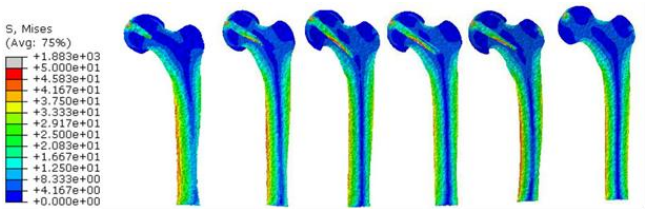


Fig. 4: Von misses stress of HRA models during normal walking conditions, (a)varus -5°,(b)straight ,(c)varus +5°,(d)sagittal +5°,(e) sagittal -5°,(f) half femur

Table 4: List of Von misses stress for each type stem malalignment for normal walking condition

Max. Von Misses Stresses (MPa)	Straight 125° (a)	Varus -5° (b)	Varus +5° (c)	Sagittal flexed +5° (d)	Sagittal extended -5° (e)	Half femur (f)
Walking	18.83	18.66	18.54	17.90	18.78	17.51

3.1.2. Hip cross section of the proximal region

The purpose to view and analyse the cross-sectional area of the proximal region is to study the Von misses stress along intact surface between the implant and femur component. Based on that, all five models show variation in the Von misses stress distribution. The cross section of the unimplanted femoral bone was also analysed. The maximum value of the Von misses stress for normal walking condition was 8.9MPa which was indicated by the varus -5° model.

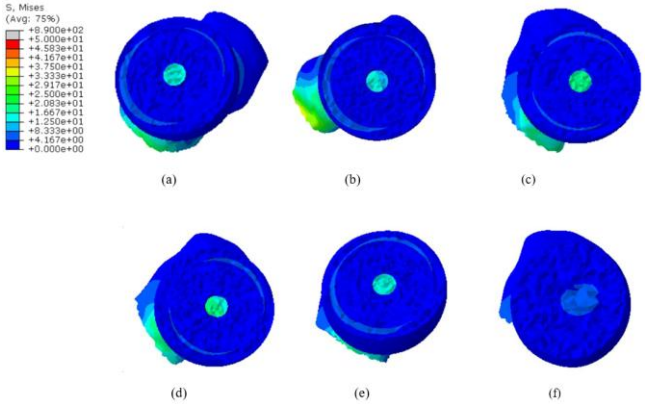


Fig. 5: Von misses stress of RHA models and half femur on the cross-section of the proximal region for normal walking condition, (a)straight,(b)varus +5,(c)varus -5d) sagittal +5,(e)sagittal-5,(f) half femur

Table 5: Maximum values of Von misses stress of HRA models and femur on the cross-section of the proximal region for normal walking condition.

Max. Von Misses Stresses (MPa)	Straight 125° (a)	Varus -5° (b)	Varus +5° (c)	Sagittal flexed +5° (d)	Sagittal extended -5° (e)	Half femur (f)
Walking	7.24	8.28	8.90	6.95	6.62	5.83

3.1.3. Hip resurfacing femoral component

Fig. 6 below shows the Von misses stress for all five malalignment-HRA models during normal walking condition. The highest maximum Von misses stress among all five models can be seen in (b) varus -5° malalignment with the value of 18.83MPa and the least value of Von misses stress is in (d) sagittal flexed +5° which has a value of 17.90MPa. The grey-coloured contour shows the maximum von misses stress resulted on the implant. The maximum value is located at the middle section on the stem and on the shell of the femoral component where the point load is applied.

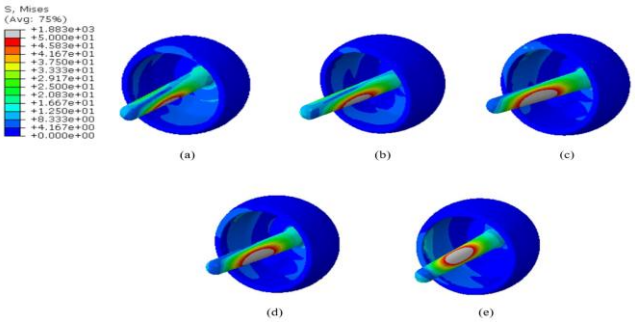


Fig. 6: Von misses stress of RHA femoral component for normal walking condition, (a)straight,(b)varus -5°, (c)varus +5°,(d)sagittal +5°,(e)sagittal -5°

Table 6: Maximum values of Von misses stress of RHA femoral component for normal walking condition.

Max. Von Misses Stresses (MPa)	Straight 125° (a)	Varus -5° (b)	Varus +5° (c)	Sagittal flexed +5° (d)	Sagittal extended -5° (e)
Walking	18.66	18.83	18.54	17.90	18.78

3.2. Effect of stem malalignment on deformation during loading transfer of HRA

3.2.1. Hip Resurfacing Arthroplasty

Fig. 7 shows the deformation of the HRA models and the half femur model during normal walking conditions. The highest deformation occurred in the sagittal extended -5° malalignment model. The maximum value achieved was 5.606 m. The red-coloured contour on the proximal region of the model shows where the maximum deformation occurs. The maximum deformation occurs at shell of the femoral component and head of the femur and decreases from the middle region to the distal region of each model.

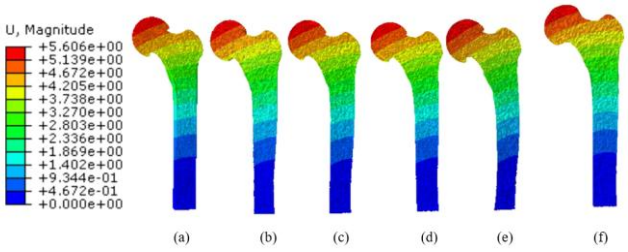


Fig. 7: Deformation of hip resurfacing femoral component during normal walking conditions, (a) Straight, (b) Varus -5°, (c) Varus +5°, (d) Sagittal +5°, (e) Sagittal -5°

Table 7: Maximum deformation on cross-section of the RHA models and femur during normal walking conditions.

Max. Von Misses Stresses (MPa)	Straight 125° (a)	Varus -5° (b)	Varus +5° (c)	Sagittal +5° (d)	Sagittal -5° (e)	Half femur (f)
Walking	5.489	5.605	5.341	5.271	5.606	17.51

3.2.2. Hip resurfacing femoral component

From the result acquired by ABAQUS software, the result of deformation of the femoral component is shown in Figure 8. The deformation of the prosthesis implant is quite small; thus, it cannot be said that it has reached the peak level of deformity. The deformation among all five HRA prosthesis implants are all moderate in value but both varus -5° and sagittal extended -5° models reached the maximum value of deformation among all models with the value of 5.616 m during normal walking conditions. The minimum value of deformity was acquired by sagittal flexed +5° model with the value of 5.276 m. Past study have also concluded that hip resurfacing has a good implant survival of 96.2% and excellent post-operative function [10]. Hence, based on the value of the maximum deformation by each model, it can be said that the values cannot lead to the biomechanical failure of the prosthesis implant. The red-coloured contour on the femoral component surface indicates where the maximum deformation occurs. Hence, the maximum deformation occurs at the outer shell surface of the femoral component and at the tip of the stem that is attached to the inside surface of the shell.

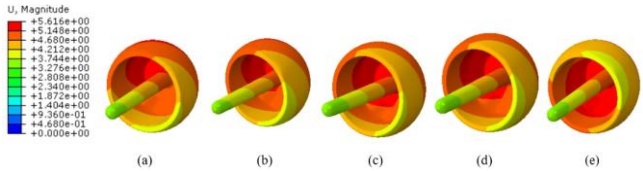


Fig. 8: Deformation of hip resurfacing femoral component during normal walking conditions, (a) Straight, (b) Varus -5°, (c) Varus +5°, (d) Sagittal +5°, (e) Sagittal -5

Table 8: Maximum deformation values in the hip resurfacing femoral component during normal walking conditions.

Max. Deformation (m)	Straight 125° (a)	Varus -5° (b)	Varus +5° (c)	Sagittal +5° (d)	Sagittal -5° (e)
Walking	5.489	5.616	5.349	5.276	5.616

4. Conclusion

The von misses stress distribution for normal walking loading conditions at the femur and femoral component was determined. The results show that for all five malalignment-HRA models, the stress distribution will not lead to the biomechanical failure of the prostheses implant and the femur. The sagittal flexed malalignment was the most stable condition during normal walking loading conditions because it achieved the lowest reading of stress distribution within the HRA model and femoral component. Furthermore, the analysis of the von misses stress for the five malalignment cases shows that the stress distribution is still below the yield strength of the femoral component which is 455MPa. Hence, this will avoid the femoral neck fracture of the hip joint from occurring. Meanwhile, for the deformation analysis of this study, again, the sagittal flexed malalignment shows the lowest value of deformation, which means under normal walking condition, at this instance of malalignment, it underwent the least deformation among all five malalignments that were analyzed. However, for further study, higher value of malalignment might affect the stress distribution and deformation which can lead to the biomechanical failure of the hip joint or dislocation of the stem implant.

References

[1] Abdullah AH, Todo M, & Nakashima Y. (2017). Prediction of damage formation in hip arthroplasties by finite element analysis using computed tomography images. *Medical engineering & physics*, 44, 8-15.

[2] Khalid MSM & Yunus R. (2012). Multiplanar reconstructed ct study of normal acetabulum-inclination angle, anteversion angle and acetabular depth (Doctoral dissertation, Universiti Sains Malaysia).

[3] McMinn D, Treacy R, Lin K & Pynsent P. (1996). Metal on metal surface replacement of the hip: Experience of the mcminn prosthesis. *Clinical Orthopaedics and Related Research*, 329.

[4] Freeman MA & Bradley GW (1983). ICLH surface replacement of the hip. An analysis of the first 10 years. *The Journal of Bone and Joint Surgery*. 65(4), 405-411.

[5] Bergmann G, Deuretzbacher G, Heller M., Graichen F, Rohlmann A, Strauss J, & Duda GN (2001). Hip contact forces and gait patterns from routine activities. *Journal of Biomechanics*, 34(7), 859-871.

[6] Kendal AR, Prieto Alhambra D, Arden NK, Carr A, & Judge A. (2016). Mortality rates at 10 years after metal-on-metal hip resurfacing compared with total hip replacement in England. Br *J Sports Med*, 50(3), 187-187.

[7] Udofia IJ, Yew A, & Jin ZM. (2004). Contact mechanics analysis of metal-on-metal hip resurfacing prostheses. *Journal of Engineering in Medicine*, 218(5), 293-305.

[8] Watanabe Y, Shiba N, Matsuo S, Higuchi F, Tagawa Y, & Inoue A. (2000). Biomechanical study of the resurfacing hip arthroplasty: Finite element analysis of the femoral component. *The Journal of Arthroplasty*, 15(4), 505-511.

[9] Bergmann G, Deuretzbacher G, Heller M, Graichen F, Rohlmann, A, Strauss J, & Duda GN. (2001). Hip contact forces and gait patterns from routine activities. *Journal of Biomechanics*, 34(7), 859-871.

[10] Shimmin AJ & Back D. (2005). Femoral neck fractures following Birmingham hip resurfacing: a national review of 50 cases. *The Journal of Bone and Joint Surgery*. 87(4), 463-464.

[11] Aulakh TS, Jayasekera N, Singh R, Patel A, Roulahamin N, Kuiper JH, & Richardson JB. (2015). Efficacy of hip resurfacing arthroplasty: 6 year results from an international multisurgeon prospective cohort study. *Acta Orthop Belg*, 81(2), 197-208.